Mesostructured Vanadium Oxide Containing Dodecylamine[⊥]

Ping Liu,[†] Igor L. Moudrakovski,[‡] Jun Liu,[§] and Abdelhamid Sayari*,[†]

Department of Chemical Engineering and CERPIC, Université Laval, Ste-Foy, Qc, Canada G1K 7P4; Steacie Institute for Molecular Sciences, National Research Council of Canada, Ottawa, Ont., Canada K1A 0R6; and Pacific Northwest National Laboratory, Richland, Washington 99352

Received January 31, 1997. Revised Manuscript Received May 14, 1997[⊗]

Two lamellar (L1, L2) and one hexagonal (H) vanadium oxide−dodecylamine mesophases have been prepared and characterized by XRD, FTIR, SEM, TEM, and NMR spectroscopy. The local environment of vanadium species was found to be controlled mainly by the synthesis temperature regardless of the nature of the mesophase. It was proposed that the structure of the final phase is governed by the acidity of the vanadium centers, and thus by the strength of the interactions between these centers and dodecylamine

Introduction

The concept of using micelles and aggregates of long-chain surfactants as templates for the synthesis of novel mesoporous silicates was first introduced by a group of scientists at Mobil in 1992.[1] Their discovery of the M41S family of silicates generated a strong interest in the use of supramolecular templates for the synthesis of periodic mesoporous inorganic materials.[2−4] In 1993, Stucky et al.[5,6] demonstrated for the first time that the same synthesis strategy can be extended to the preparation of mesoporous metal oxides and metallophosphates, among others. By an appropriate use of the charge balance between surfactant ions and charged inorganic species, they succeeded in preparing three-dimensionally structured tungsten, lead, antimony, and iron oxides. However, none of these materials was stable upon removal of the template. Moreover, they found that most of the non-silica-based materials had a strong tendency to form lamellar structures.[5]

Using similar approaches based on electrostatic interactions, several groups succeeded in preparing mesostructured W,[7] Sn,[8] Zr,[9−11] V,[12] Hf,[13] and Al[14] oxides as well as Ti,[15] Zr,[9,16] Al,[17−19] and V[20,21] metallophosphates. After removal of the surfactants, the porous structure was preserved only in the case of Zr and Al oxides and Ti and Zr phosphates. The strategy involving electrostatic forces between the template and the inorganic species thus met limited success in the synthesis of thermally stable non-silica mesoporous materials.

It was mentioned in the literature that the neutral templating approach using amines or nonionic polymer surfactants as templates can be used to generate non-silica mesoporous materials.[22] This was confirmed recently on the preparation of mesoporous alumina in the presence of poly(ethylene oxide) surfactants.[23] The alumina thus prepared was thermally stable and exhibited a high surface area with narrow pore size distribution.

Recently, Antonelli and Ying[24−27] developed a synthetic route referred to as ligand-assisted templating approach. According to the authors, this method involves the formation of a nitrogen−metal covalent bond to initiate the organization of surfactant−metal oxide mesophase. This method is promising, since the tem-

[⊥] Published as NRCC No. 40830.
[†] Université Laval.
[‡] Steacie Institute for Molecular Sciences.
[§] Pacific Northwest National Laboratory.
* To whom correspondence should be addressed. Tel: +1-418656 3563. Fax: +1-418-656 5993. E-mail: sayari@gch.ulaval.ca.
[⊗] Abstract published in *Advance ACS Abstracts,* August 1, 1997.

(1) Kresge, C. T.; Leonowicz, M. E.; Roth, W. J.; Vartuli, J. C.; Beck, J. S. *Nature* **1992**, *359*, 710.
(2) Sayari, A. *Stud. Surf. Sci. Catal.* **1996**, *102*, 1.
(3) Zhao, X.; Liu, G. Q.; Millar, G. J. *Ind. Eng. Chem. Res.* **1996**, *35*, 2075.
(4) Sayari, A. *Chem. Mater.* **1996**, *8*, 1840.
(5) Huo, Q.; Margolese, D. I.; Ciesla, U.; Demuth, D. G.; Feng, P.; Gier, T. E.; Sieger, P.; Firouzi, A.; Chmelka, B. F.; Schüth F., Stucky; G. D. *Chem. Mater.* **1994**, *6*, 1176.
(6) Ciesla, U.; Demuth, D.; Leon, R.; Petroff, P. M.; Stucky, G.; Unger, K.; Schüth, F. *J. Chem. Soc., Chem. Commun.* **1994**, 1387.
(7) Stein, A.; Fendorf, M.; Jarvie, T. P.; Mueller, K. T.; Benesi, A. J.; Mallouk, T. E. *Chem. Mater.* **1995**, *7*, 304.
(8) Ulagappan, N.; Rao, C. N. R. *Chem. Commun.* **1996**, 1685.
(9) Ciesla, U.; Schacht, S.; Stucky, G. D.; Unger, K. K.; Schüth, F. *Angew. Chem., Int. Ed. Engl.* **1996**, *35*, 541.
(10) Kim, A. Y.; Bruinsma, P. J.; Shen, Y. L.; Liu, J. *Mater. Res. Soc. Symp. Proc.* **1996**, *435*, 131.
(11) Reddy, J. S.; Sayari, A. *Catal. Lett.* **1996**, *38*, 219.
(12) Luca, V.; MacLachlan, D. J.; Hook, J. M.; Withers, R. *Chem. Mater.* **1995**, *7*, 2220.
(13) Liu, P.; Liu, J.; Sayari, A. *Chem. Commun.* **1997**, 577.
(14) Vaudry, F.; Khodabandeh, S.; Davis, M. E. *Chem. Mater.* **1996**, *8*, 1451.
(15) Antonelli, D. M.; Ying, J. Y. *Angew. Chem., Int. Ed. Engl.* **1995**, *34*, 2014.
(16) Liu, P.; Reddy, J. S.; Sayari, A. *Mater. Res. Soc. Symp. Proc.* **1996**, *431*, 101.
(17) Oliver, S.; Kuperman, A.; Coombs, N.; Lough, A.; Ozin, G. A. *Nature* **1995**, *378*, 47.
(18) Chenite, A.; Le Page, Y.; Karra, V. R.; Sayari, A. *J. Chem. Soc., Chem. Commun.* **1996**, 413.
(19) Sayari, A.; Moudrakovski, I.; Reddy, J. S.; Ratcliffe, C. I.; Ripmeester, J. A.; Preston, K. F. *Chem. Mater.* **1996**, *8*, 2080.
(20) Abe, T.; Taguchi, A.; Iwamoto, M. *Chem. Mater.* **1995**, *7*, 1429.
(21) Doi, T.; Miyake, T. *Chem. Commun.* **1996**, 1635.
(22) Tanev, P. T.; Pinnavaia, T. J. *Science* **1995**, *267*, 865.
(23) Bagshaw, S. A.; Pinnavaia, T. J. *Angew. Chem., Int. Ed. Engl.* **1996**, *35*, 1102.
(24) Antonelli, D. M.; Ying, J. Y. *Angew. Chem., Int. Ed. Engl.* **1996**, *35*, 426.
(25) Antonelli, D. M.; Ying, J. Y. *Chem. Mater.* **1996**, *8*, 874.
(26) Antonelli, D. M.; Nakahira, A.; Ying, J. Y. *Inorg. Chem.* **1996**, *35*, 3126.
(27) Antonelli, D. M.; Ying, J. Y. *Curr. Opinion Colloid Interface Sci.* **1996**, *1*, 523.

S0897-4756(97)00067-7 CCC: $14.00

plate could be readily removed by low-temperature extraction using a mixture of nitric acid and 2-propanol. Niobium[24,25] and tantalum[26] oxides with very high surface area and an ordered mesoporous structure have been prepared using this method.

Since vanadium oxides and phosphates are extremely important in catalysis and in advanced materials applications, considerable effort has been devoted to the synthesis of vanadium substituted zeolites[28] and mesoporous silicate molecular sieves,[29,30] as well as pure vanadium oxides[12,31] and vanadophosphates.[20,21] Luca et al.[12] reported the first example of mesoporous vanadium oxide with a three-dimensional structure. They first reacted cetyltrimethylammonium (CTMA) chloride and ammonium vanadate. The CTMA vanadate thus formed was dissolved in ethanol and titrated to a pH of 2.2. This gave a precipitate with an XRD pattern similar to MCM-41 type materials. However, the material was found to be thermally unstable. More recently, Janauer et al.[31] used the reaction between dodecyltrimethylammonium bromide and V_2O_5 to generate a new mesolamellar vanadium oxide. Short-chain diamines and aromatic amines have also been used as templates for hydrothermal synthesis of novel vanadium oxides.[32,33]

Here we report on the synthesis of mesostructured vanadium oxides using dodecylamine as template. These materials were characterized using IR, XRD, TEM, and ^{13}C, ^{14}N, ^{15}N, and ^{51}V NMR.

Experimental Section

The starting materials used in the preparation of mesostructured vanadium oxide samples were oxovanadium triisopropoxide (Strem) and dodecylamine (Aldrich). In a typical synthesis of mesostructured vanadium oxide, 1.46 g of $C_{12}H_{25}NH_2$ was dissolved in 5 g of ethanol. To this solution, 3.81 g of $VO(O^iPr)_3$ was added. This mixture was stirred for 10 min before 15 g of water was slowly added. A brown precipitate was formed immediately which was then aged at room temperature typically for 24 h. This may be followed by a hydrothermal treatment at 373 K for 24 h in a Teflon-lined autoclave. The product was filtered and washed with water and ethanol and dried at room temperature.

X-ray diffraction patterns were obtained on a Siemens D5000 diffractometer, using Cu Kα radiation. Transmission electron micrographs (TEM) were recorded using a JEOL 1200 instrument operated at 120 kV. All the TEM samples were prepared by sonicating the dry powder in distilled water for a few minutes. A drop of thus formed suspension was placed on a TEM grid covered with a thin carbon film and dried in air. FTIR spectra were obtained on a Nicolet Magna-IR 550 spectrometer using the KBr pellet technique. Scanning electron microscopy (SEM) images were recorded on a JEOL 840A microscope operating at an accelerating voltage of 10 kV.

^{51}V MAS NMR spectra were obtained on a Bruker AMX-300 and a Bruker MSL-200 spectrometers at 7.05 and 4.7 T (frequencies 78.8 and 52.6 MHz, respectively), equipped with Bruker high-speed 4 mm MAS probe. The speed of rotation was 10−15 kHz, and synchronization of the acquisition with the spinner rotation was used to reduce distortion of the spectra. All spectra were obtained using single-pulse excitation with a pulse width of 0.5 μs ($\pi/12$ for liquid) and 1 s acquisition delay.

The isotropic chemical shifts reported here were corrected for second-order quadrupolar-induced shifts and given relative to the external reference $VOCl_3$. The correction was done based on measurements made at two different fields. Analysis of the spectra was performed using the WINFIT simulation package from Bruker. The chemical shift anisotropy parameters were estimated by fitting the most intensive spinning sidebands from the central transition (undisturbed by the quadrupole interactions to first order) to a pure chemical shift anisotropy (CSA) pattern. Estimates of the quadrupole coupling constants C_Q were obtained from the field dependence of the signals.

^{13}C and ^{15}N NMR spectra were obtained with cross-polarization and magic angle spinning (CP MAS) on a Bruker AMX-300 instrument (75.5 and 30.1 MHz, respectively). Speed of rotation was 3 kHz, the CP contact time was 2 and 5 ms for ^{13}C and ^{15}N, respectively. ^{14}N NMR spectra were recorded at 21.7 MHz on a AMX-300 instrument using a quadrupole echo pulse sequence ($\pi/2$ pulse of 5 μs and delays of 50 and 55 μs were employed). Signals from liquid tetramethylsilane (TMS) and the NO_3^- group in solid NH_4NO_3 were used as external references.

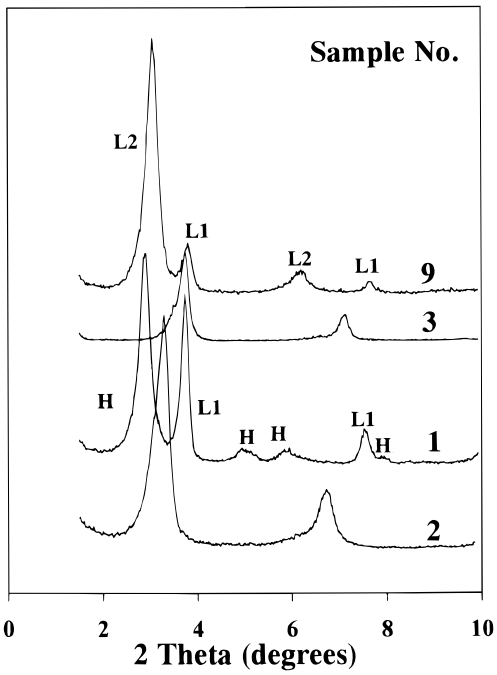

Figure 1. XRD patterns of typical as-synthesized samples. Figures on the right-hand side indicate the sample numbers given in Table 1.

Results and Discussion

Synthesis of Mesostructured Vanadium Oxide. In previous reports on the preparation of vanadium oxide, V_2O_5 was used as the vanadium source and short-chain amines or long-chain ammonium salts were used as templates or intercalates.[31−33] Here, we used a long-chain primary amine as template. $VO(O^iPr)_3$ was hydrolyzed in the presence of the surfactant, leading to the formation of different phases of nanocomposites, depending on the synthesis conditions.

Table 1 lists the gel composition, synthesis time, and temperature as well as the final morphology of the products as indicated by XRD. Figure 1 shows typical XRD patterns of the resultant phases. There are essentially three different phases consisting of a hexagonal ($d_{100} = 3.0$ nm) and two lamellar ($d_{001} = 2.3$ nm,

(28) Sayari, A.; Moudrakovski, I. L.; Ratcliffe, C. I.; Ripmeester, J. A.; Preston, K. F. In *Synthesis of Microporous Materials: Zeolites, Clays and Nanostructures*; Occelli, M. L., Kessler, H., Eds.; Marcel Dekker: New York, 1996; p 417.
(29) Reddy, K. M.; Moudrakovski, I. L.; Sayari, A. *J. Chem. Soc., Chem. Commun.* **1994**, 1059.
(30) Reddy, J. S.; Liu, P.; Sayari, A. *Appl. Catal.* **1996**, *148*, 7.
(31) Janauer, G. G.; Dobley, A.; Guo, J.; Zavalij, P.; Whittingham, M. S. *Chem. Mater.* **1996**, *8*, 2096.
(32) Zhang, Y.; Haushalter, R. C.; Clearfield, A. *Chem. Commun.* **1996**, 1055.
(33) Zhang, Y.; O'Connor, C. J.; Clearfield, A.; Haushalter, R. C. *Chem. Mater.* **1996**, *8*, 595.

Table 1. Synthesis Conditions and Structure of Vanadium Oxide-Docedylamine Mesophases

sample no.	gel composition surfactant	$VO(O^iPr)_3$	EtOH	H_2O	time [a] (h)	temperature (K)	phase structure
1	0.5	1	7	52	24	300	H, L1
2	0.5	1	7	52	24 + 24	300 + 373	L2
3	0.5	1	54	344	24 + 72	300 + 373	L1
4	0.5	1	217	11	24	300	L2
5	0.25	1	7	52	18	300	L1, U
6	0.25	1	7	52	18 + 48	300 + 373	L2
7	1	1	7	52	24	300	L2
8	1.5	1	7	52	24	300	L2
9	0.5	1	7	52	0		L2, L1
10	0.5	1	7	52	72	300	H, L1
11	0.5	1	7	–[c]		300	L2
12	0.5	1	5.4[d]	52	24	300	L2, L1
13	0.5	1	7	52	24	273	L2

[a] The plus (+) sign stands for "followed by"; (b) H: hexagonal (d = 3.0 nm), L1: lamellar (d = 2.3 nm); L2: lamellar (d = 2.8 nm), U: unknown (d = 3.0 nm); (c) hydrolyzed by moisture from air; (d) 2-propanol.

2.8 nm) phases. They will be referred to as H, L1, and L2, respectively. As seen in Table 1, the morphology of the final phase depends strongly and in a complex way on the synthesis conditions used. Up to now, conditions for the formation of pure L1 and L2 phases have been identified; however, whenever H formed, it was always mixed with L1 phase.

Figure 2 shows the transmission electron micrographs (TEM) of L1 (sample 3 in Table 1) and L2 (sample 11) lamellar phases and a mixture of the hexagonal H and the lamellar L1 phases (sample 1). As seen, the lamellar phases were of good quality and their d distances determined by TEM were consistent with XRD data. However, it was difficult to observe the H phase in sample 1 by TEM even though its XRD pattern exhibits, in addition to the main (100) peak, well resolved (110), (200), and (210) peaks, similar to those of MCM-41 silicates.

Effect of Surfactant to Vanadium Ratio. The $C_{12}H_{25}NH_2$/V ratio was varied from 0.25 to 1.5 while the amounts of ethanol and water were kept constant. At a ratio of 0.25, a mixture of the L1 phase and an unknown phase U with d_{100} = 3.0 nm was obtained after aging for 18 h at room temperature (Table 1, sample 5). This mixture was converted to the lamellar phase L2 after being heated at 373 K for 48 h (sample 6). At a ratio of 0.5, aging at room temperature for 24 or 72 h led to the formation of a mixture of L1 and the hexagonal phase H (samples 1 and 10). However, when the solid phase was separated immediately after precipitation, i.e., without aging, it consisted of a mixture of L1 and L2 phases (sample 9). This indicates that a phase transformation from L2 to H may have occurred during room-temperature aging. Prolonged aging (144 h) at the same temperature (sample 1A, not shown in Table 1) did not induce further transformation, and the relative amounts of L1 and H as shown by XRD were found to be unchanged. Further increase of the surfactant to vanadium ratio led at room temperature to the exclusive formation of pure L2 phase (sample 7).

Effect of Ethanol to Water Ratio. Several samples were prepared using different ethanol to water ratios while keeping the surfactant to vanadium ratio constant at 0.5 and the synthesis temperature at 300 K. When no ethanol was used, dodecylamine was warmed to about 50 °C in the presence of $VO(O^iPr)_3$ followed by adding water. The product obtained was a mixture of L1 and L2. At a ratio of 0.135, a mixture of H and L1 was formed (Table 1, sample 1). Increasing the ratio to 20 gave a pure L2 phase (sample 4). When no water was added, hydrolysis of the organometallic species with air moisture diffusing into the ethanol solution also gave the pure L2 phase (sample 11). Moreover, the use of 2-propanol as the solvent instead of ethanol (2-propanol/water = 0.104) afforded a mixture of L1 and L2 phases (sample 12). We also used methanol as the solvent. After 30 min stirring with $VO(O^iPr)_3$, a yellow precipitate which was attributed to $VO(OMe)_3$ dimer was observed.[34] Addition of dodecylamine and water also led to the formation of a mixture of L1 and L2 phases.

Effect of Temperature. An experiment was conducted at 273 K to investigate the effect of temperature on the morphology of the final mesophase (sample 13). A pure L2 phase was found, while the solid material formed at room temperature from the same starting ratios contained a mixture of L1 and H (sample 1). This mixture can be converted to the L2 phase after heat treatment at 373 K (sample 2).

The complex relationship between the morphology of organic–inorganic mesophases and the synthesis conditions is difficult to unravel. The formation of the H phase was possible only in the presence of ethanol as the solvent. Attempts have been made to remove the surfactant from materials with three-dimensional structure (H). Both calcination at 773 K and extraction with a mixture of ethanol and HCl resulted in the collapse of the structure.

Structural Characterization. The FTIR spectra for four representative vanadium oxide samples are shown in Figure 3. The two samples prepared at 373 K (samples 2 and 3) exhibited similar spectra with two absorption bands at about 1000 and 960 cm^{-1}. The absorption at ca. 1000 cm^{-1} was associated with the V=O bond.[31] It is known that V_2O_5 displays three major absorption peaks at 617, 827, and 1022 cm^{-1}. The first two bands were assigned to the vibrations of $-V-O-V-$ and $O-(V)_3-$, respectively.[31] The assignment of the band at 960 cm^{-1} is still controversial. In some reports, it was considered as characteristic of the decavanadate anion $V_{10}O_{28}^{6-}$.[35] Because they did not observe such an absorption band, Luca et al.[12] used this assignment to argue that their mesostructured vanadium oxide sample was reminiscent of V_2O_5 and not decavanadate salt

(34) Bradley, D. M.; Mehrotra, R. C. *Metal Alkoxides*; Academic Press: New York, 1977.
(35) Day, V. W.; Klemperer, W. G.; Maltbie, D. J. *J. Am. Chem. Soc.* **1987**, *109*, 2991.

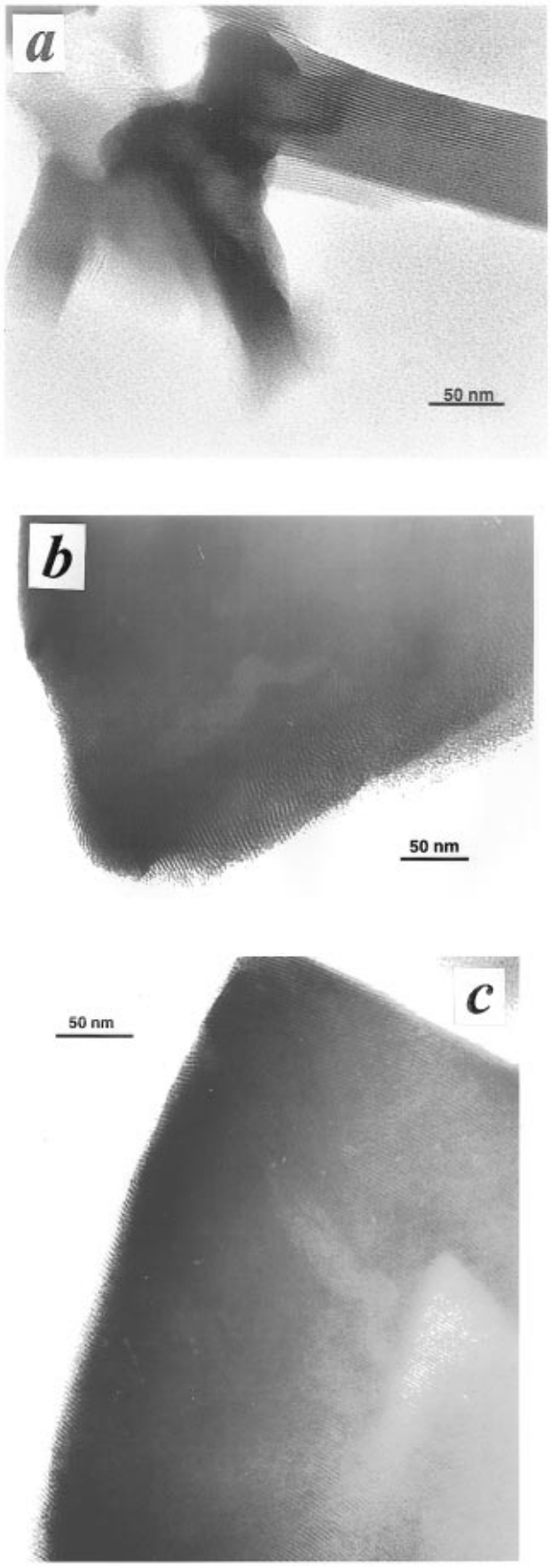

Figure 2. Transmission electron micrographs of (a) L1 phase (sample 3 in Table 1), (b) L2 phase in sample 11, and L1 phase in sample 1.

which, similarly to mesostructured tungsten oxide, might be comprised of unconnected Keggin ions forming cavities where the surfactant resides.[7] However, in a recent report on mesolamellar vanadium oxide, Janauer et al.[31] considered this band to be the same as the 1022 cm^{-1} band of V_2O_5 shifted to a significantly lower wavenumber. They argued that the corresponding lengthening of the V═O bonding may be related to additional bond at the position of either O or V.

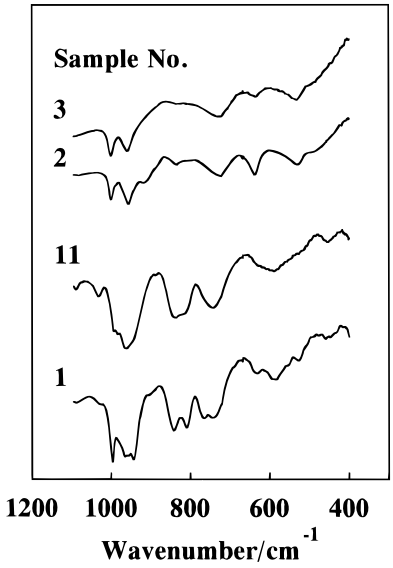

Figure 3. Infrared spectra of representative samples. Figures on the left-hand side indicate the sample numbers given in Table 1.

As seen in Figure 3, the two materials prepared at room temperature (Table 1, samples 1 and 11) also exhibited similar IR absorption spectra. However, the relative intensity of the peak at 1000 cm^{-1} was lower than that of materials obtained at 373 K. In addition, both spectra showed a broad and intense absorption at around 960 cm^{-1}. This may indicate that there are several slightly different vanadium environments in the inorganic parts of the mesophase. Considering the discrepancy in the assignment of the 960 cm^{-1} IR absorption band, it would be too speculative to discuss further the vanadium environment based on IR data only. However, as documented hereafter ^{51}V NMR enabled us to distinguish between different vanadium species.

Typical ^{51}V MAS NMR spectra and their parameters are shown in Figure 4 and Table 2, respectively. On the basis of the similarity between their NMR data, the samples can be divided into two groups consisting of samples 1 and 11 on one hand and samples 2 and 3 on the other. This grouping, which is also reflected in the FTIR data, coincides with the difference in their synthesis temperature 300 vs 373 K. The ^{51}V NMR spectra of samples 1 and 11 were dominated by the line with a chemical shift at about −503/−507 ppm. Two other lines with lower intensity, one shifted to higher and the other to lower field, were also observed. All three lines had similar chemical shift anisotropies and moderate quadrupolar constants of 3−5 MHz. Note that the low-intensity line in the low field (chemical shift at about −425 ppm) has the largest values for quadrupolar coupling constant and asymmetry parameter. In addition to the line at ca. −505 ppm, samples 2 and 3 (L2 and L1, respectively) exhibited two signals, both in the higher field range. All signals had chemical shift anisotropies in the range 300−400 ppm, and were characterized by fully asymmetric tensor of the chemical shift.

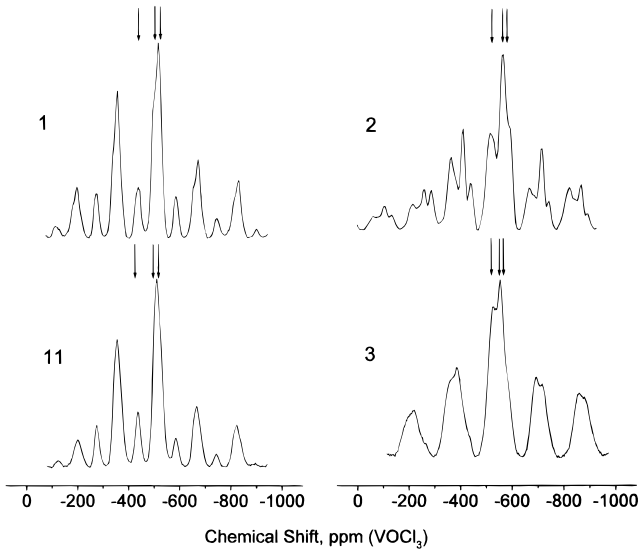

Figure 4. ^{51}V MAS NMR spectra of representative samples. Figures on the left-hand side indicate the sample numbers given in Table 1.

Table 2. ^{51}V MAS NMR Data for Representative Mesostructured Vanadium Oxide Samples

sample no.	$\delta_{iso.}$, ppm (± 5)	relative intensity, %	$\Delta\delta$, ppm (±30)[a]	C_Q, MHz
1	−425	21	−400	5.1 ± 0.4
	−507	57	−350	4.2 ± 0.3
	−520	22	−350	3.5 ± 0.3
11	−421	20	−400	4.9 ± 0.5
	−503	69	−350	4.2 ± 0.3
	−525	11	−350	3.6 ± 0.3
2	−507	43	−370	2.9 ± 0.3
	−556	42	−350	2.5 ± 0.3
	−583	15	−300	2.8 ± 0.4
3	−504	63	−370	3.1 ± 0.3
	−552	19	−350	3.0 ± 0.3
	−579	18	−300	3.4 ± 0.3

[a] $\Delta\delta = |\delta_3 - \delta_{iso.}|$, Parameters of asymmetry η were found to be 0.5 ∼ 0.6 for all the lines, except for the one with a chemical shift at around −425 ppm, where $\eta \approx 0.9-1$.

It is well established that the type and magnitude of the chemical shift anisotropy strongly correlate with the type and the extent of association of vanadium−oxygen polyhedra.[36] Thus, vanadium in strongly distorted tetrahedral sites with adjacent VO_4 tetrahedra sharing two oxygen atoms (sites of Q^2 type) is typically characterized by a fully anisotropic chemical shift tensor ($\eta \neq 0$) with anisotropy in the range 200−400 ppm. The metavanadate of monovalent metals, whose crystal structures contain infinite chains of corner-sharing VO_4 tetrahedra, is one example of such systems. All of these materials show CSA in the range 200−400 ppm,[36] while the parameter of asymmetry lays within 0.3−0.7.[36,37] On this basis, it may be concluded that all the signals with isotropic chemical shifts between −500 and −600 ppm belong to VO_4 tetrahedra with two common oxygen atoms between adjacent VO_4 groups, which are the main building units in the samples. Another fact that illustrates the resemblance between the vanadium coordination in our materials and those in metavanadates is the closeness of the observed quadrupole coupling constants to those reported for metavanadates, which are normally between 3 and 4.2 MHz. The appearance of several lines with different isotropic chemical shifts is most likely due to some differences in the composition of the second coordination sphere of vanadium. Differences in the detailed structure of the vanadium−oxygen tetrahedra seem to be relatively small. This is inferred from the rather small variations of the ^{51}V NMR parameters for the different sites. Since the line at ca. −500 ppm is present for all samples and none of the other lines is specific for any particular phase, it appears that the structure of the oxide framework is governed not by some particular VO_4 tetrahedra but rather by their different mutual arrangements. The relatively low accuracy of the quantification poses significant limitations for further discussion of this subject. Nevertheless, on the basis of the above arguments, it seems that the nature of the V species depends essentially on the synthesis temperature but not on the final morphology.

An interesting observation is the line at about −420 ppm for samples 1 and 11. The position of the signal together with other magnetic resonance parameters distinguish it from the others and suggests somewhat different local environment for vanadium in these sites. To our knowledge, isotropic chemical shifts for vanadium−oxygen polyhedra (VO_4 and VO_6) were never observed in the field below −480 ppm.[36] Obviously, we should seek an explanation of a such large observed shift in an interaction of vanadium−oxygen units with the molecules of template. The lower symmetry of the vanadium environment would reflect in higher C_Q and η, which we indeed observe. Actually, it is likely that this line is also present in the spectra of samples 2 and 3 but, because of its low intensity, is hidden underneath neighboring broad lines and by spinning sidebands.

As mentioned above, Luca et al.[12] prepared mesostructured vanadium oxide using CTMA chloride and ammonium vanadate. Their ^{51}V NMR data showed essentially an axially symmetric species with $\delta_{11} = \delta_{22} = -341$ ppm, $\delta_{33} = -1043$, and isotropic chemical shift at −618 ppm. These parameters are characteristic of V_2O_5-like species with V in square-pyramidal or distorted octahedral environment. Notice that these parameters, particularly if the δ_{33} is corrected using the value of the isotropic chemical shift, are almost identical with those of bulk V_2O_5. In addition, this material had a XRD pattern similar to that of MCM-41 type hexagonal structure with $d_{100} = 3.6$ nm, and its FTIR spectrum had no band at 960 cm^{-1}. All these findings indicate that the material described by Luca et al.[12] is different from those reported here. Moreover, the layered material prepared by Janauer et al.[31] using V_2O_5 and dodecyltrimethylammonium bromide is also different from the L1 and L2 lamellar phases described in this work. It would be interesting to undertake further work to compare all these vanadium oxide based materials.

Morphology

FTIR and ^{51}V NMR data indicated clearly that the local structure of our materials is governed by the synthesis temperature regardless of the "crystalline" structure as revealed by XRD. The four samples (samples 1, 2, 3, and 11) selected for comparative study by FTIR and ^{51}V NMR were also investigated by SEM. Although all of the samples exhibited different morphologies, features consistent with lamellar structures such as sheets and platelike particles were easily

(36) Lapina, O.; Mastikhin, V.; Shubin, A.; Krasilnikov, V.; Zamaraev, K. *Prog. NMR Spectrosc.* **1992**, *24*, 457.

(37) In ref 35, the authors used non standard notations for the CSA. These were adapted to common solid-state NMR notations, where $\Delta\delta = |\delta_3 - \delta_{iso}|$, and $|\delta_3 - \delta_{iso}| > |\delta_1 - \delta_{iso}|$, $|\delta_2 - \delta_{iso}|$.

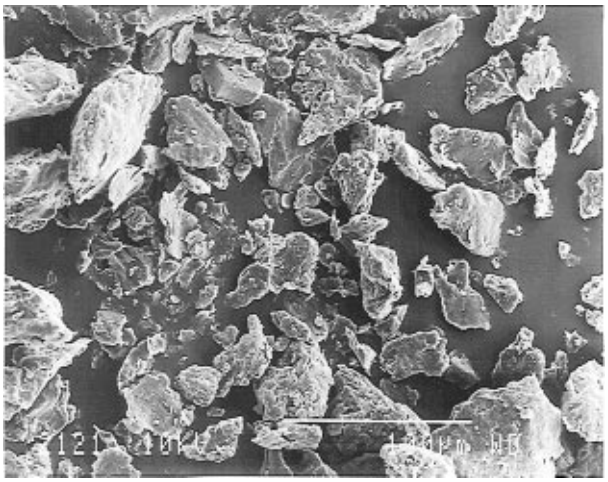

Figure 5. SEM mcirograph of sample 11.

detectable in each case. Figure 5 is a typical electron micrograph for sample 11. This material consisted of simple particles displaying a layered topology. Sample 1 was comprised of flat particles either dispersed (Figure 6a) or assembled in a spongelike way to form intricate three-dimensional particles 50−100 μm in size (Figure 6b). The closeup view of one such particle (Figure 6c) shows that the primary particles are flat with up to 20 μm in length and 2 μm in width.

In addition to simple layered particles, similar to those shown in Figure 5, sample 3 was made up of sheets that self-assembled into aggregates the shape of which strikingly mimics roses, with beautiful precision (Figure 7a). Even more surprising, as shown in Figure 7b, these roses, each 10−15 μm in diameter, assembled into bunches. Sample 2 presented the most diverse morphological features. As shown in Figure 8a, it exhibited essentially three types of particles: (i) microrods up to 200 μm in length, (ii) flat platelets with a squarelike shape, 5−20 μm in dimension, and (iii) 3D particles, up to 100 μm in size, comprised of an intricate network of interconnected rods. Figure 8b,c show that the microrods are multilamellar in nature with either flat or cylindrical shapes. The closeup view of a 3D particle provided in Figure 8d shows the complex architecture of the interconnected microrod networks as well as the presence of the small flat particles.

The interpretation of the physical origins underlying the formation of such diverse morphologies remains a challenging issue. This is however a valuable addition to the growing list of unique shapes and forms reported recently for silica and aluminophosphate mesophases prepared in the presence of surfactants.[38−44]

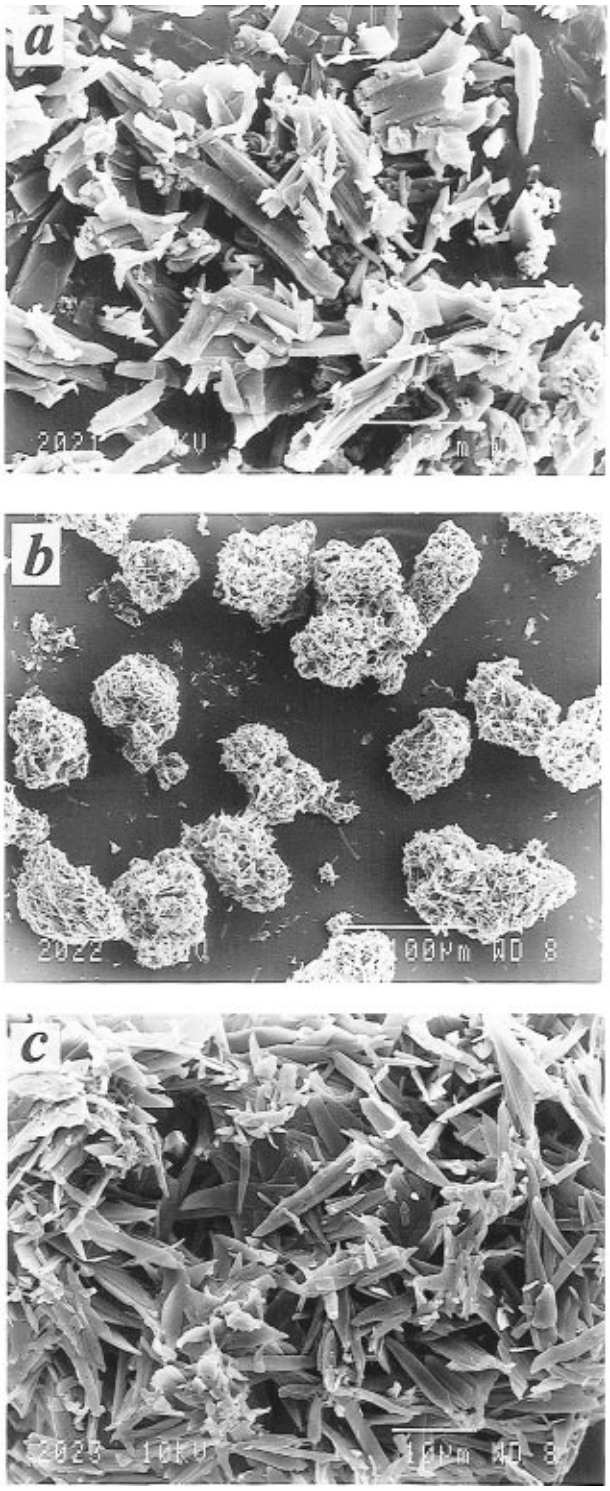

Figure 6. SEM micrographs of sample 1.

Formation Mechanism

Recently, Antonelli and Ying[24−26] developed the ligand-assisted templating mechanism which is based on the formation of a metal−nitrogen covalent bond between the surfactant primary amine and metal alkoxides (Nb and Ta ethoxides). Considering the fact that our synthesis procedure is quite similar to that of mesoporous Nb and Ta oxides, it would be interesting to see if such a mechanism also applies to the current system.

The solution chemistry of oxovanadium isopropoxide and amines has received little attention in the literature. It is known that the O^{i}Pr groups may be readily exchanged by O or N donors,[34] indicating a rather weak interaction between V and O^{i}Pr. In particular, the O^{i}Pr groups can be easily exchanged with −OMe, −OEt and other alkoxyl groups. As far as the interaction between V and amine group is concerned, it is reasonable to assume that it depends strongly on the acidity

(38) Chenite, A.; Le Page, Y.; Karra, V. R.; Sayari, A. *J. Chem. Soc., Chem. Commun.* **1996**, 411.
(39) Lin, H. P.; Mou, C. Y. *Science* **1996**, *273*, 765.
(40) Schacht, S.; Huo, Q.; Voigt-Martin, I. G.; Stucky, G. D.; Shüth, F. *Science* **1996**, *273*, 768.
(41) Oliver, S.; Kuperman, A.; Coombs, N.; Lough, A.; Ozin, G. A. *Nature* **1995**, *378*, 47.
(42) Tanev, P. T.; Pinnavaia, T. J. *Science* **1996**, *271*, 1267.
(43) Yang, Y.; Coombs, N.; Ozin, G. A. *Nature* **1997**, *386*, 692.
(44) Huo, Q. S.; Feng, J. L.; Shüth, F.; Stucky, G. D. *Chem. Mater.* **1997**, *9*, 14.

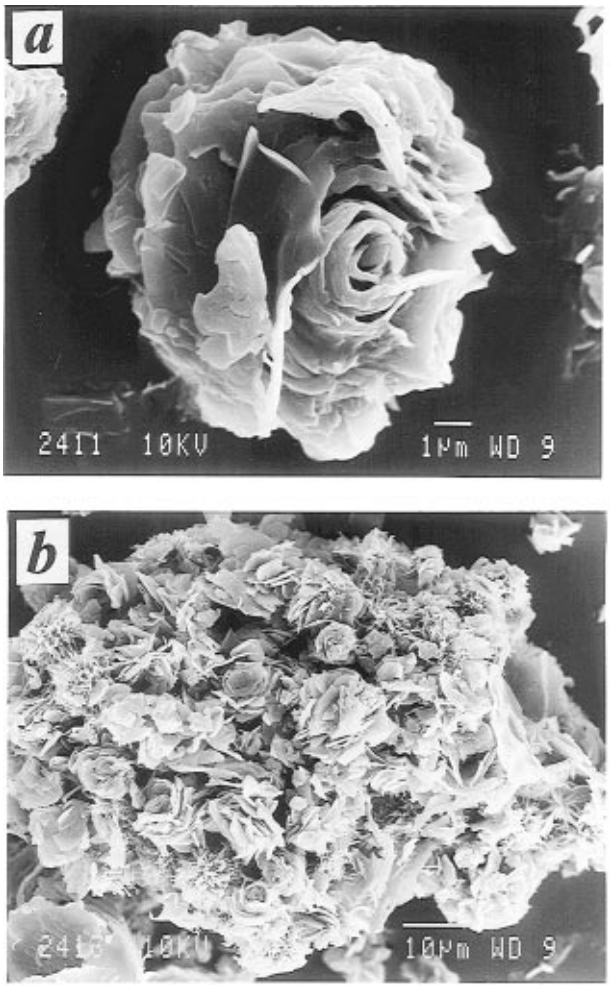

Figure 7. SEM mcirographs of sample 3.

of the vanadium center. Moreover, depending on the strength of such interactions, the vanadium species may or may not be considered as part of the headgroup of the amphiphile molecule. This has direct implications on the packing factor g[45] and thus on the morphology of the organic−inorganic mesophase. The packing factor is defined as $g = V/a_0l$, where a_0 is the headgroup area, and V and l designate the volume and the critical chain length of the hydrocarbon chain. For $^1/_2 < g < 1$, the formation of a bilayer and thus an organic−inorganic lamellar phase is favored. In contrast, for $^1/_3 < g < ^1/_2$, the formation of cylindrical micelles leading to a hexagonal organic−inorganic mesophase is preferred. If the vanadium center interacts strongly with the amine, it will become part of the headgroup, thus decreasing g which, in turn, favors the formation of the H phase. This was indeed the case when ethanol which leads to $VO(OEt)_3$ with enhanced acidity was used. On the contrary, in the event of weak interaction, the headgroup remains small and therefore lamellar phases are favored. Several experimental observations are consistent with this proposal. For example, in the presence of an equimolar mixture of $VO(O^iPr)_3$ and acetylacetone or tributylamine instead of pure $VO(O^i\text{-}Pr)_3$, only the L1 lamellar phase was generated at room temperature. It is believed that the V complexes formed after reaction with acetylacetone or tributylamine have a diminished acidity and therefore interact less strongly with dodecylamine.

(45) Israelachvili, J. N. *Intermolecular and Surface Forces*; Academic Press: London, 1992; Chapter 17.

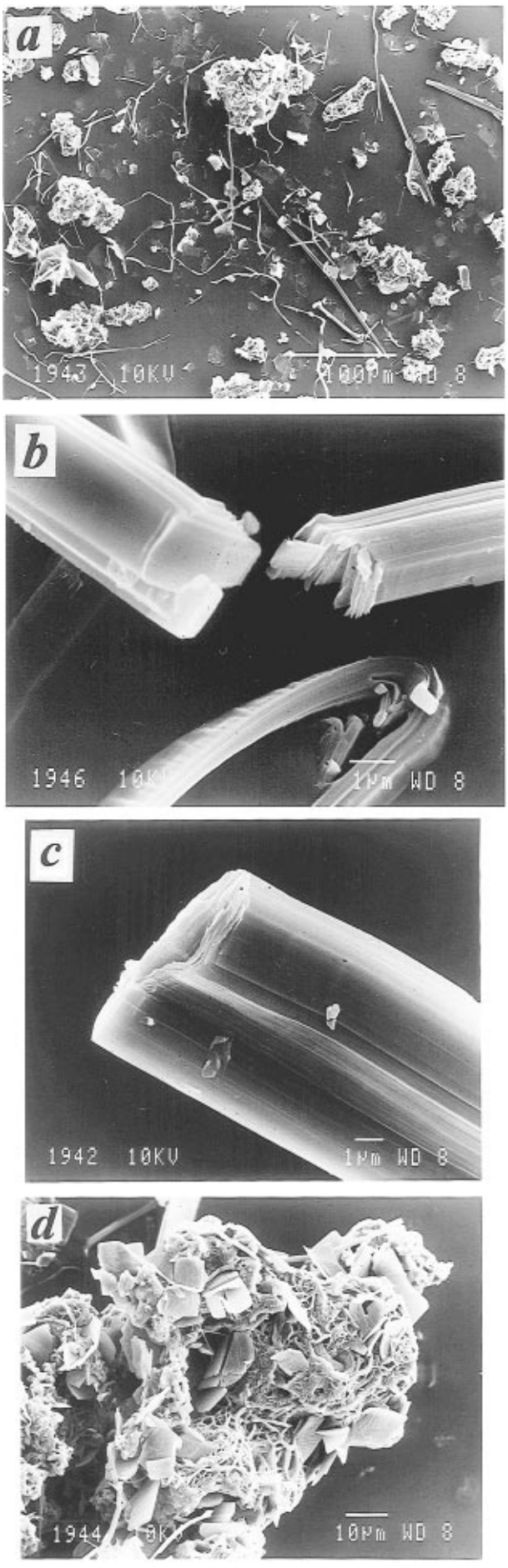

Figure 8. SEM micrographs of sample 2.

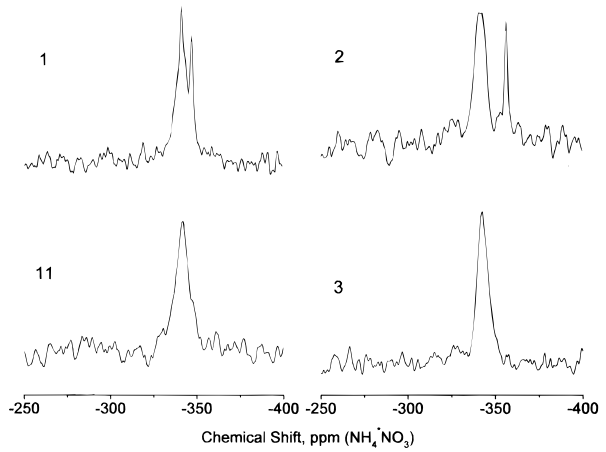

Figure 9. ^{15}N CPMAS NMR spectra of representative samples. Figures on the left-hand side indicate the sample numbers given in Table 1.

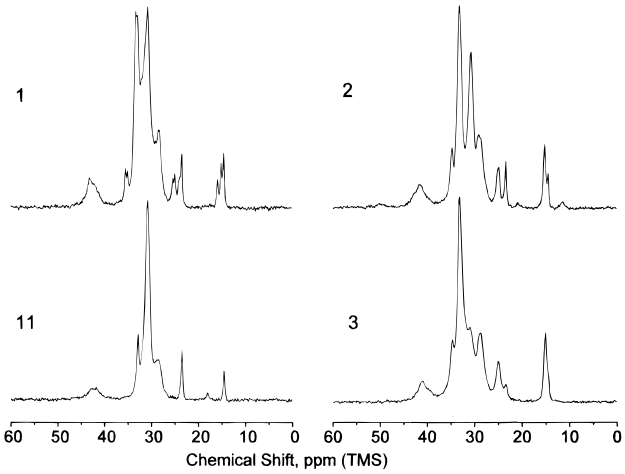

Figure 10. ^{13}C CPMAS NMR spectra of representative samples. Figures on the left-hand side indicate the sample numbers given in Table 1.

Additional support to our proposal may also be sought in ^{13}C, ^{14}N, and ^{15}N NMR data for the surfactant occluded in the as-synthesized materials. Figures 9 and 10 show the ^{15}N and ^{13}C CP MAS NMR spectra of representative samples. Relevant NMR parameters are collected in Table 3. These data are to be compared with those for pure solid dodecylamine for which we found that the ^{15}N isotropic chemical shift was -346.0 ppm and the ^{13}C chemical shift of the C_1 carbon of the alkyl group was -43.1 ppm.[19] In the case of lamellar aluminophosphate mesophases prepared in the presence of dodecylamine at pH of ca. 3, the ^{15}N NMR signal shifted downfield to -340.0 ± 0.4 ppm, and that of the ^{13}C signal of the C_1 shifted to 40.2 ± 0.4 ppm indicating that protonation of the amine group has occurred.[19] The formation of a nitrogen−metal (i.e., tantalum or niobium) covalent bond in the ligand-assisted mechanism was also postulated mostly on the basis of ^{15}N CP MAS NMR data.[24,25] In this case, a downfield shift of ca. 7 ppm between solid dodecylamine and the organic−inorganic mesophase was observed in addition to extensive broadening believed to be due to the effect of ^{93}Nb ($I = {}^9/_2$) or ^{181}Ta ($I = {}^7/_2$) quadrupole. In the present work, because of line broadening, it was not always possible to associate a ^{13}C signal to a ^{15}N signal stemming from the same occluded surfactant molecules. Nevertheless, Table 3 shows that within the mesophase there exist different interactions between the surfactant and the inorganic walls. Moreover, only for samples containing the H phase was there a distinct ^{15}N NMR signal at ca. -340.7 indicating the occurrence of a strong interaction, conceivably in the form of a N−V covalent bond. ^{14}N NMR data provide indirect evidence for such a proposal. Sample 1 (phases H + L1) and sample 7 (phase L2) were selected for ^{14}N NMR studies. Immediately after synthesis, the solids were filtered without washing and spectra were recorded using the wet solids and the liquid filtrates. No ^{14}N NMR signals could be detected in any of these experiments. It is well-known that because of the large quadrupole constant of the ^{14}N isotope, ^{14}N NMR spectra of amines are very sensitive to the symmetry of the nitrogen environment. Generally, only spectra of protonated amines with nitrogen in tetrahedral environment are observed.[46,47] Extensive broadening of NMR lines for nonprotonated amines with long aliphatic chain makes them in most cases, unobservable. The signal is even less likely to be detected when the mobility of the amine is limited or when some distribution of the amine environment is present. In the current situation, since no ^{14}N NMR signals could be detected, it can be safely concluded that the interaction between the occluded amine and the inorganic walls inferred by ^{13}C and ^{15}N NMR data is not a simple protonation.

Table 3. ^{15}N and $^{13}C_1$ CP MAS NMR Data for Representative Mesostructured Vanadium Oxide Samples

sample no.	phase	^{15}N, ppm	$^{13}C_1$, ppm[a]
1	H, L1	−340.6	42.0 (51)
		−346.5	43.2 (49)
11	L2	−341.8	41.6 (23)
			42.8 (77)
1A[b]	H, L1	−340.8	41.8 (39)
		−346.7	43.2 (61)
2	L2	−342.1	39.9 (7)
		−356.0	41.5 (82)
			43.0 (11)
3	L1	−342.6	39.5 (22)
			41.2 (70)
			42.5 (8)

[a] Numbers in parentheses indicate the relative intensity of the NMR signals; (b) prepared as sample 1 except that it was aged at room temperature for 144 h instead of 24 h.

In conclusion, we prepared and characterized three new vanadium oxide−dodecylamine mesophases. It is proposed that the acidity of the V centers in the alkoxide plays a key role regarding the nature of the mesophase morphology. As the acidity decreases, the interaction between the amine surfactant and the vanadium alkoxide decreases, leading to a smaller average headgroup area, thus to a higher g factor. These events favor the formation of lamellar phases.

CM970067U

(46) Chen, C. Y.; Burkett, S. L., Li, H. X.; Davis, M. E. *Mesoporous Mater.* **1993**, *2*, 27.
(47) Tanev, P. T.; Pinnavaia, T. J. *Science* **1995**, *267*, 865.